A NEUTRAL HYDROGEN SURVEY OF M31

BRETT YANG

School of Physics and Astronomy

The University of Manchester

Third Year Laboratory Report

14 December 2018

ABSTRACT

21cm observations over 57 points indicate (1) the majority of HI content is contained within a radius of 10.1kpc showing a ring-like structure and (2) the rotation curve is proximately flat in the outer region up to 25kpc. The latter implies a linear increase in dynamical mass even in regions with negligible HI density. The total dynamical mass is 2 orders of magnitude greater than the observed HI mass.

1. INTRODUCTION

The Andromeda galaxy has been broadly observed in the 21cm hydrogen spectra line. Its proximity and abundance in neutral hydrogen provide an excellent opportunity to study its properties by means of neutral hydrogen distribution, mass distribution and rotation curve. There have been several surveys of the neutral hydrogen in M31 in the past, including those of Roberts [1], Guibert [2], synthesis observations by Emerson [3], and more recent kinematics analysis by Braun [4]. The study of M31 can provide understandings in other spiral galaxies as well as a guidance to understand the Milky Way.

The data presented in this report was collected using the 76m Lovell radiotelescope at Jodrell Bank Observatory. The observations were carried out in the form of grid scans on the 15th March 1992, a total of 57 spectra were produced over the period of 24 hours, all points of observation are separated by $\Delta\alpha = 2'$ in right ascension and $\Delta\delta = 20'$ in declination. The antenna beam width is 46" in right ascension and 11'35" in declination. Each spectrum consists 512 channels, each has a width of 6.35kHz. This report will first explore some useful physical background, then discuss the data reduction procedures and present processed data in the form of contour maps, from which the neutral hydrogen distribution and dynamical mass distribution will be deduced. A comparison between the total neutral hydrogen mass and the total dynamical mass will lead to understandings of the structure of M31.

2. BACKGROUND THEORY

The transition of spin state in hydrogen atoms emits radiation at 1.42GHz (21cm hydrogen line). Radiation at this frequency is capable of penetrating dust clouds as it propagates towards the Earth, thus the effect of extinction can be neglected.

2.1 HI Mass

The total neutral hydrogen mass can be calculated from column density N_h and the total projected area A_{proj}.

HI column density measures the number of hydrogen atoms projected along the line of sight and is directly related to the spectral brightness:

$$N_h = 3.848 \times 10^{14} \int T_b(\alpha, \delta, v) dv \ \ [cm^{-2}]$$

where T_b is the brightness temperature and v is the frequency. The integral can be calculated by means of moment analysis. The zeroth moment gives the weighted mean intensity:

$$\int T_b(\alpha, \delta, v) dv \ \equiv \sum_{i=1}^{n} I_i(\alpha, \delta)$$

where $I_i = T_b \Delta v$ is the specific intensity within each channel with velocity width Δv.

The total projected area A_{proj} can be derived using Euclidean geometry. In equatorial coordinate system, the declination angle $\delta\ [Hr: Min: Sec]$ has a projecting effect on right ascension $\alpha\ [Deg: ArcMin: ArcSec]$. The correction for this effect when calculating the angular separation is:

$$\Delta\alpha(\delta) = \frac{\alpha_2 - \alpha_1}{\cos\delta}$$

For a given angular separation $\Delta\theta\ [rad]$, its projected length at a line-of-sight distance $D\ [cm]$ is given by:

$$L = 2D \tan\frac{\Delta\theta}{2}\ [cm]$$

2.2 Rotation Curve

If the gravitational potential of a spiral galaxy is approximately symmetric about the centre, the rotational velocity v_{rot} is only a function of radial distance R. Under the assumption of spherical symmetry, the gravitational acceleration is $\frac{GM(R)}{R^2}$ and the rotational velocity can be found by equating central force:

$$v_{rot} = \sqrt{\frac{GM(R)}{R}}$$

When observing galaxies at an inclination angle i, the observed component of rotational velocity is projected by a factor of $\sin i$ as illustrated in the Figure 1. Another correction is needed for points

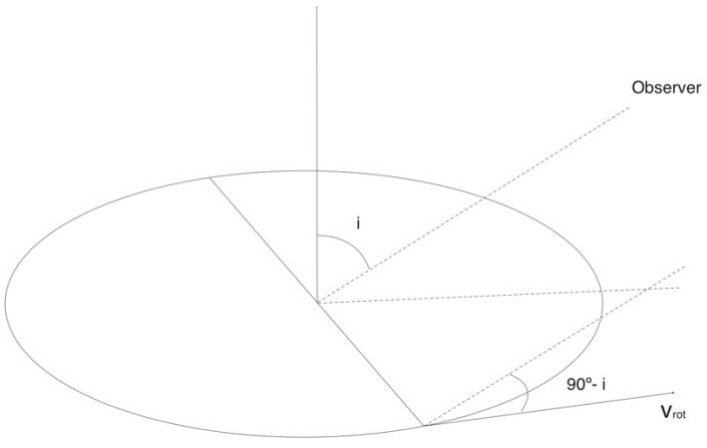

Figure 1 The rotational velocity at inclination as seen by an observer

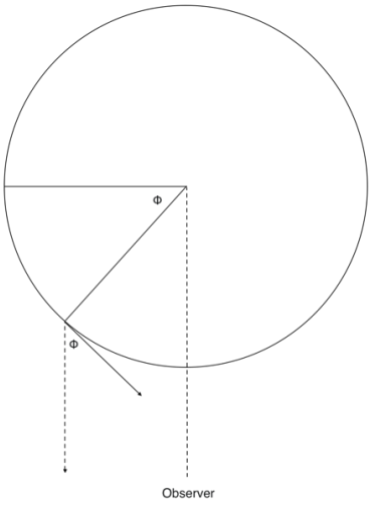

Figure 2 Rotational velocity seen by observer at an angle from major axis

which are off the major axis on the projected area. As shown in Figure 2, the observed component is projected by a factor of $\cos\phi$, where the azimuthal angle ϕ is measured from the major axis about the centre. The systemic velocity v_{sys} of the system is not affected.

The observed velocity is the sum of the systemic velocity and the projected rotational velocity:

$$v_{obs} = v_{sys} + v_{rot}\cos\phi\sin i$$

This gives the scaling relation between observed velocity and rotational velocity:

$$v_{rot} \propto v_{obs} \propto \sqrt{\frac{M(R)}{R}}$$

3. DATA REDUCTION

The data collected from the Jodrell Bank centre undertook an initial noise reduction by means of frequency methods. The process removes several noise features, but further corrections are necessary for sensible data analysis. All post-observation data corrections were carried out within the software package DRAWSPEC [5].

3.1 Baseline Removal

On the spectra line data (intensity vs doppler velocity), the baseline takes a parabolic shape. As opposed to expected trend of zero flux everywhere except for regions: (1) the doppler velocity $v_{doppler} \approx 0$, where neutral hydrogen line from the Milky Way shows a predominant peak. (2) a distinguished curve within the range $600 \lesssim v_{obs} \lesssim 0\ km.s^{-1}$, where the neutral hydrogen in M31 dominates.

The parabolic baseline amplifies spectral line near its local maximum and depletes the spectral line elsewhere, thus it is important to reduce the effect to the minimum. Because of the parabolic nature of the baseline, a polynomial fit to appropriate regions of the spectra is sufficient. Small noise peaks ($Tdv \sim 0.5\ K.km.s^{-1}$) distant from regions of hydrogen line are manually removed.

3.2 Local Hydrogen Removal

In general, contribution from local hydrogen is approximately gaussian on the spectra, distributed around $v_{obs} = 0$. For most spectra, local hydrogen contribution is well separated from that of M31. The local hydrogen peaks were removed to a good accuracy by gaussian subtraction. In the outer ring of M31 where points of observation fall in the range $41º45'00'' < \delta < 42º30'00''$ and $44'00'' < \alpha < 48'00''$, the rotational velocities, v_{rot}, are large along the line of sight (away from Earth) and cancel out the systemic velocity v_{sys} (towards Earth), resulting in the merge of two spectral lines. In these cases, gaussian subtraction is performed by iteration, using fits from neighbouring points where only horizontal velocity component contributes to v_{rot}.

3.3 Scaling Data

At low elevation angles, the receiving area of the telescope is distorted sufficiently by its own mass to have a notable effect on the telescope gain. In order to limit the percentage error to less than 1%, the brightness temperature needs to be calibrated for spectra with elevation $el < 25º$. The gain elevation relation for the Lovell telescope was used to correct the observed brightness temperature.

The raw spectra were calibrated with reference to a noise source, but in practice the flux units are arbitrary. Since the brightness temperature scales linearly with blackbody temperature at radio frequencies, by comparing the observed flux for a known astronomical source (S8) with standard result, the scale factor was calculated to be $a = 0.648$.

3.4 Organisation of Data

It is necessary to convert data to the optimal forms in order to serve the interests of this experiment.

The zeroth moment $Mom0 = \sum_{i=1}^{512} I_i(\alpha, \delta) = 158.6\ [K.km.s^{-1}]$ was obtained from the calibrated spectra. A contour map for this quantity is shown in Figure 3 from which the total hydrogen mass can be deduced.

Provided the reduced spectra are approximately gaussian, the 1st moment corresponds to the intensity weighted mean velocity. The 1st moment was calculated to be $Mom1 = \frac{\sum_{i=1}^{512} I_i(\alpha,\delta)\times v_i}{\sum_{i=1}^{512} I_i(\alpha,\delta)} = -188.537\ [s^{-1}]$. Figure 4 presents a contour map showing the velocity field.

4. LARGE SCALE FEATURES

Having calibrated and organised the raw data to more comprehensive forms, the quantities of interests can be extracted analytically.

4.1 Neutral Hydrogen Distribution

Figure 3 presents an intensity map of neutral hydrogen at each angular position. The most striking feature of the contour is the two nearly axisymmetric intensity peaks. Despite a high inclination of 77º from edge-on position, these peaks on the contour suggests that the majority of HI mass is distributed in ring-shaped region. The peak regions are located at a distance of $10.1kpc$ from the centre. In the region enclosed by the ring structure, the contour lines are close to evenly spaced. This implies a relatively uniform mass distribution of the inner region. In regions outside the ring structure, the spacing between contour lines becomes comparatively larger and vanishes further out. Evidently, HI mass is contained within the ring structure and the region enclosed by it.

From the weighted mean intensity obtained in Section 3.4 and the number density equation in Section 2.1, the HI column number density was calculated to be $N_h = 2.894 \times 10^{20}\ [cm^{-2}]$. Due to the limitations of DRAWSPEC, the total projected area of M31 cannot be directly obtained from Figure

3. Given all points of observations on the grid scan are equally separated, the total projected area can be estimated in a similar fashion as Riemann sum. The grid was divided into 43 rectangular boxes of the same dimensions. Using standard result [6] for the distance to M31, $D = 780 \pm 40\ [kpc]$ and taking into account the effect of declination on equatorial coordinates, the projected dimensions for each rectangular box were calculated: $d_\alpha = 2.783 \times 10^{22}\ [cm]$ and $d_\delta = 1.400 \times 10^{22}\ [cm]$. This is under the assumption that line-of-sight distance does not vary with angular position, this results in an extra error of $\Delta D = 2.9\ [kpc]$.

The total projected area was calculated to be $A_{proj} = 1.676 \times 10^{46}\ [cm^2]$. Hence the total mass of neutral hydrogen is:

$$M_{h,M31} = N_h \times A_{proj} = (8.100 \pm 0.891) \times 10^{39}\ [kg]$$

Expressed in solar mass $M_{h,M31} = (4.072 \pm 0.448) \times 10^9\ M_\odot$. The associated errors arise from baseline removal, $\Delta(Tdv) = 3.2\ [K.km.s^{-1}]$ and standard result for distance to the M31, $\Delta D = 40 + 2.9 = 42.9\ [kpc]$.

4.2 Dynamical Mass

Figure 4 presents the contour map for the velocity field of M31. As discussed in Section 4.1, the HI mass is concentrated within a radial distance of $10.1kpc$ from the centre. The proximately uniform mass distribution in the central region implies spherical symmetry, from which it follows the rotational velocity takes the form as one described in Section 2.2. Near-uniform mass distribution also indicates that the distance-dependent total mass $M(R) \propto R^3$, the scaling relation between rotational velocity and radius is thus $v_{rot} \propto R$. As the region outside the ring structure does not depend on $M(R)$, a scaling relation of $v_{rot} \propto \sqrt{\frac{1}{R}}$ is expected.

As shown in Figure 5, the rotation curve of M31 was plotted for 7 points up to a radius of $23.46kpc$. Data points were taken along the major axis of contour plot in Figure 4 to avoid the complication by the azimuthal angle discussed in Section 2.2. The rotation curve shows a linear trend up to $R{\sim}10kpc$ as expected, however, the curve flattens out at $v_{rot}{\sim}259\ km.s^{-1}$ for $R > 10kpc$ as opposed to the expected Keplerian decline. The flat rotation curve implies linear increase in mass $M(R) \propto R$ up to a $R{\sim}25kpc$. The total dynamical mass at this distance was calculated taken into account associated errors from $\Delta v_{rot} = 1\ km.s^{-1}$ and $\Delta R = 2\ kpc$:

$$M_{Dyn,M31} = \frac{(v_{max})^2 R_{max}}{G} = (7.753 \pm 0.698) \times 10^{41}\ [kg]$$

In terms of solar mass, $M_{Dyn,M31} = (3.899 \pm 0.351) \times 10^{11} M_\odot$.

This result is two orders of magnitude larger than $M_{h,M31}$, its implications are not clear. However, it is reasonable to postulate the existence of an 'invisible' matter which resides in the outer disk of M31.

5. Conclusions

This survey has measured rotation curve out to $R{\sim}25kpc$. The rotation curve does not show signs of decline as opposed to previous studies [4]. The total dynamical mass cannot be accounted for by total HI mass. The nature of the contributors is yet understood but its existence proves necessity for further studies.

Reference

[1] M. S. Roberts, "The hydrogen distribution in galaxies," in *International Astronomical Union. Symposium No. 31*, H. v. Woerden, Ed., London, Academic Press, 1967, p. 189.

[2] J. Guibert, "A neutral hydrogen survey of the Andromeda Nebula," *Astronomy and Astrophysics Supplement*, vol. 12, p. 263, 1973.

[3] D. T. Emerson, "High Resolution Observations Of Neutral Hydrogen In M31 - I: The Overall Distribution," *Monthly Notices of the Royal Astronomical Society*, vol. 169, no. 3, pp. 607-629, 1974.

[4] R. Braun, "The Distribution And Kinematics Of Neutral Gas In M31," *The Astrophysical Journal*, vol. 372, pp. 54-66, 1991.

[5] H. Liszt, *DRAWSPEC*, Charlottesville: H. S. Liszt, 1994.

[6] A. Pedlar, "The Mass and Hydrogen Content of M31," University of Manchester, Manchester, 2013.

[7] D. Morin, Introduction to Classical Mechanics: With Problems and Solutions, Second Edition ed., Cambridge University Press, 2008, p. 690.

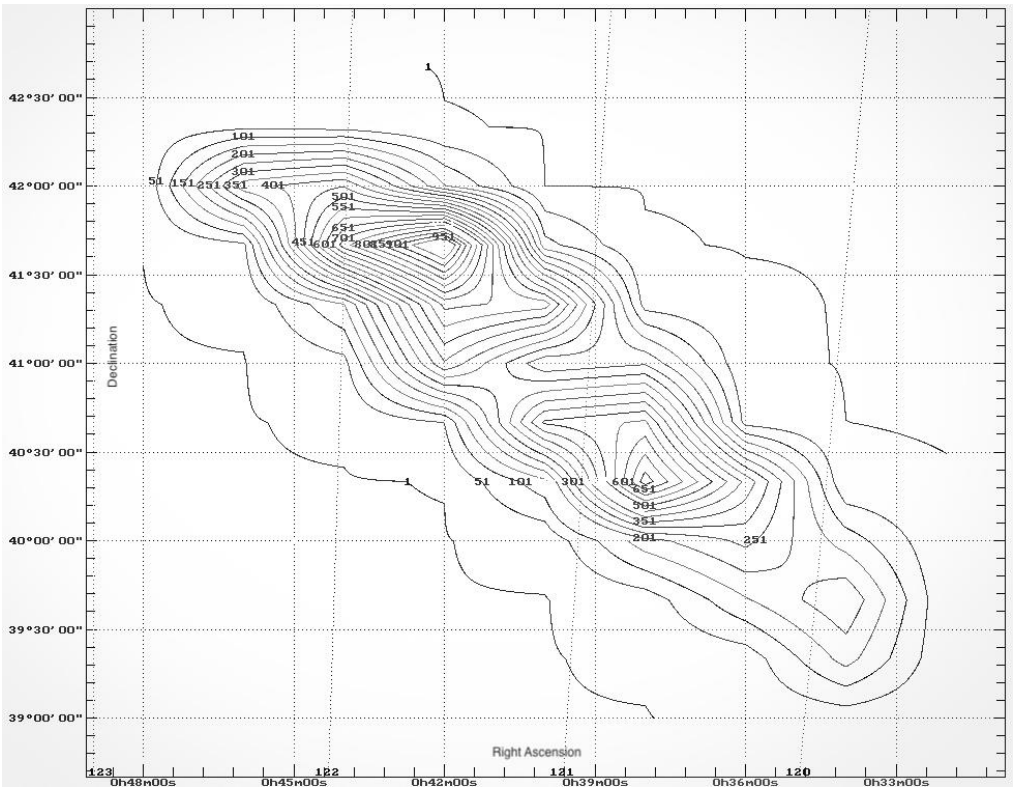

Figure 3 Distribution of 21cm HI line from M31. The quantity plotted is the integrated intensity at each angular position, in units of [K.km.s^{-1}]. The ring structure of neutral hydrogen is seen at the two brightness peaks

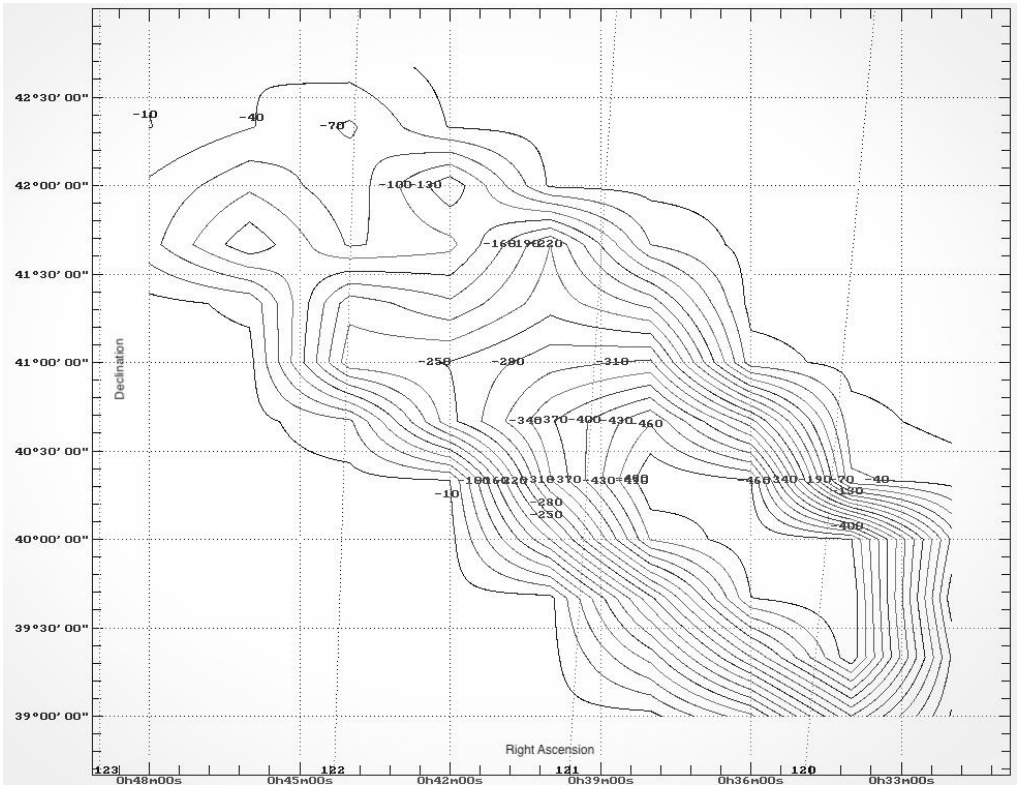

Figure 4 Contour map showing mean velocity as function of position. The plot resembles a 'spider diagram' close to the centre.

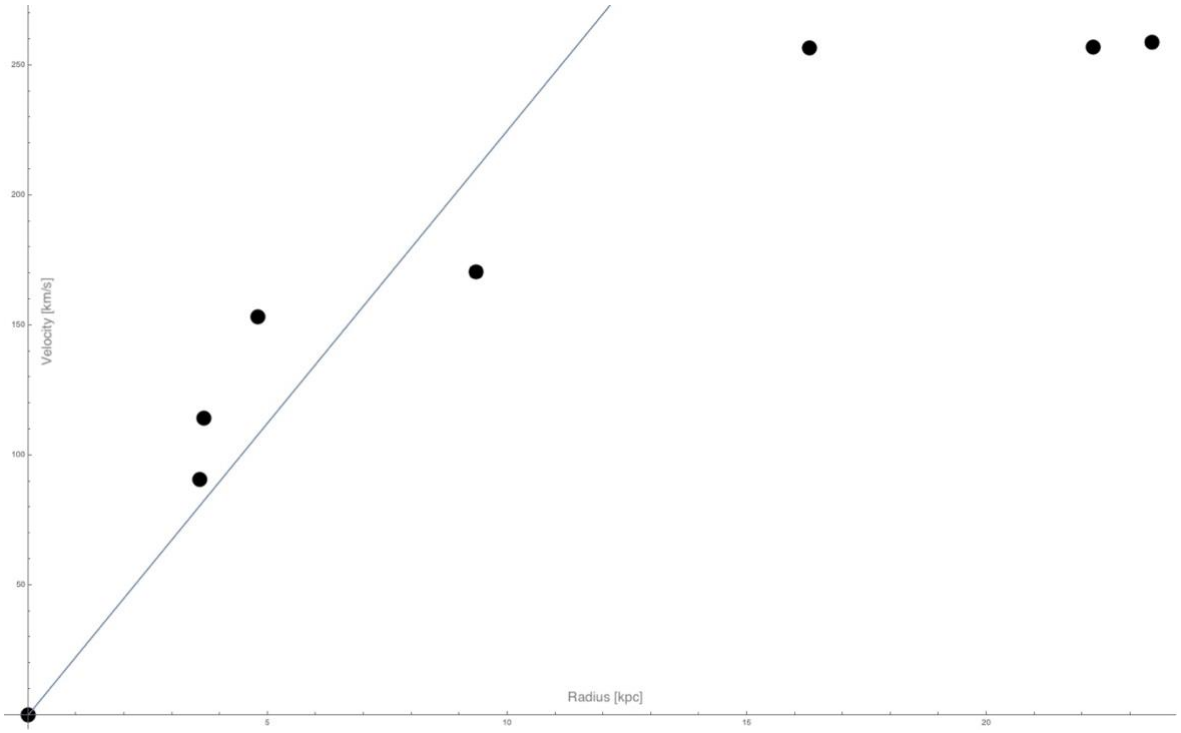

Figure 5 Rotational velocity at 7 distinct radial distances. Linear trend is seen up to $R = 10.1\ kpc$.